Spin exchange between a quantum well and the donor layer in $Si/Si_{1-x}C_x$

H.-J. Kümmerer, K. Hüftle, C. Weinzierl, and G. Denninger*
2. Physikalisches Institut, Universität Stuttgart, Pfaffenwaldring 57, D-70550 Stuttgart, Germany

N. Nestle
Universität Ulm, Sektion NMR, D-89069 Ulm, Germany

K. Eberl
MPI für Festkörperforschung, Heisenbergstrasse 1, D-70569 Stuttgart, Germany
(Received 15 December 1998)

Electron-spin-resonance (ESR) data from modulation-doped $Si/Si_{1-x}C_x$ heterostructures are reported. The experiments at high ESR frequency (94 GHz) and corresponding high magnetic field (3.5 T) enabled us to separate the ESR of the conduction electrons in the quantum well from the ESR of the phosphorous donors in the doping layer. At temperatures above 20 K a thermally activated electron-exchange process between the quantum well and the donor layer is observed. The effective activation energy of this process is ≈ 19 meV. The g factors of the conduction electrons and of the P donors were determined with high absolute accuracy. [S0163-1829(99)02319-X]

I. INTRODUCTION

Two-dimensional electron gas (2DEG) systems are of increasing importance in semiconductor physics and in technical applications. Due to the confinement of the electrons in one dimension and due to the possible lattice strain, the electronic band structure is considerably different from the band structure of the bulk material. This has direct effects on properties like the electronic bandgap, the effective masses of the charge/spin carriers, and the electronic g factors. The $Si/Si_{1-x}C_x$ material system has become available only recently,[1–5] and is particularly suited for electron-spin-resonance (ESR) investigations, due to small hyperfine couplings and small g-factor deviations from the free-electron value. Direct ESR investigations of the quantized electrons in 2DEG's are complementary to electrical transport and optical experiments. In a first ESR investigation of the 2DEG in the $Si/Si_{1-x}C_x$ system,[6] we were able to analyze the ESR intensity in terms of contributions both from the quantum well and from the Si:P donor layer. However, a direct spectral resolution of the two spin systems was not possible so far, since the difference in the resonance positions was smaller than the resonance linewidth. Even with a good signal-to-noise ratio of the ESR signal, a deconvolution into two contributions is numerically unstable. In this contribution we show that doing the ESR experiments at high field ($B \approx 3.5$ T, $f_{\mu w} \approx 94$ GHz, W-band) yields decisive advantages.

The two spin systems (quantum well, P-doping layer) are clearly resolved in resonance position, due to the difference in the respective g factors. There is direct experimental evidence of a coupling between these two spin systems. ESR offers the rather unique property to investigate these dynamic exchange processes in a time window that is both too fast for electrical transport investigations and too slow for optical experiments.

In this contribution we will concentrate on this specific sensitivity of ESR to dynamic electron/spin exchange. A prerequisite of such experiments is the ability to do ESR at high fields (and high frequencies) on rather large, thin, conducting semiconductor samples. Since commercial ESR resonators at 94 GHz cannot even accommodate these samples and are not optimized for conducting samples anyhow, the construction of a suitable probehead was the basis for the experiments. This is discussed in more detail in the experimental section.

II. SAMPLE

The main property of the sample is the existence of a two-dimensional electron gas that is achieved by a multilayer structure grown on a ≈ 0.5-mm thick Si wafer: The quantum well is formed in a 6-nm thick $Si_{0.99}C_{0.01}$ layer, sandwiched between two 3-nm thick Si spacer layers. The electrons are supplied by a 6-nm thick Si layer doped with P ($4 \cdot 10^{18}$ cm^{-3}, areal density $2.4 \cdot 10^{12}$ cm^{-2}). This layer sequence is repeated 10 times in our sample to increase the signal strength. Due to the different lattice constants, the $Si_{1-x}C_x$ layer is under strong tensile biaxial strain, which leads to a massive deformation of the bandstructure of this whole $Si/Si_{1-x}C_x$ heterostructure. The two conduction band Δ valleys in the growth direction are lowered in energy, and the band offset for the electrons is of the order of 50 meV for every percent C alloyed into the Si.[7]

The electrons for the quantum well are supplied from the P-donor layers. Assuming a bandstructure of the P-induced impurity band according to calculations,[8] and an energy position of $E_0 \approx 7$ meV for the first subband (6-nm well width, $m_{\parallel}^* = 0.19\ m_0$, $m_{\perp}^* = 0.92\ m_0$), we arrive at an energy diagram as shown in Fig. 1. At $T = 0$ K, approximately 65% of the electrons are in the quantum well, and the Fermi energy is -32 meV (measured from the conduction band edge). The quantum well is filled with a concentration $n_e = 1.56 \cdot 10^{12}$ cm^{-2}. The spatial separation of the two systems is only ≈ 3 nm, and the spin systems are coupled by

 ©1999 The American Physical Society

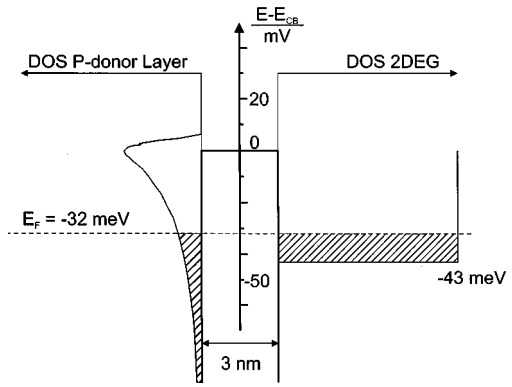

FIG. 1. Energy-band diagram of the $Si/Si_{1-x}C_x$ quantum-well sample. The density of states (DOS) is depicted in relative units for the quantum well and for the Si:P donor layer.

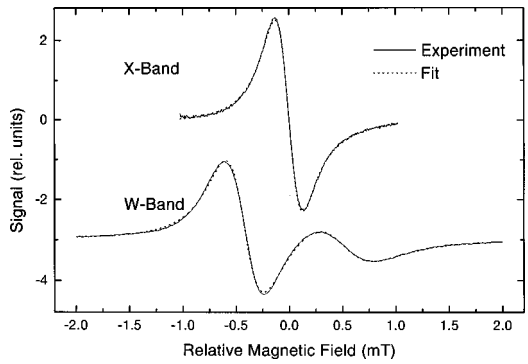

FIG. 2. X-band ESR spectrum $f_{\mu w}=9.365707$ GHz. Field offset: 335.136 mT; temperature: 6.0 K; power: 52 mW; model used for fit: two Lorentzian lineshapes without dispersion contribution. W-band ESR spectrum $f_{\mu w}=93.97$ GHz. Field offset: 3360.6 mT; temperature: 5.8 K; power: 0.6 mW; model used for fit: two Lorentzian lineshapes with equal dispersion contribution.

tunneling and/or by thermal activation over the barrier of ≈ 30 meV.

III. EXPERIMENTAL SETUP

The measurements were performed using a high-field EPR spectrometer (W-Band, 94 GHz), consisting of a heterodyne setup of the two microwave bridges Bruker ESP 900-1041 and ER 041 XG, which can deliver up to 5 mW microwave power.

A helium-flow cryostat (Oxford CF 1200, temperature range from 4.2 to 350 K) is mounted in the room-temperature bore of a superconducting magnet (solenoid type, 8 T maximum field). For standard ESR experiments the magnet is operated in persistent mode and the necessary sweep of the magnetic field is realized by additional superconducting sweep coils with a sweep width of ± 800 G. The temperature of the sample was measured by a Lakeshore Cernox temperature sensor with an accuracy of ± 0.2 K. The small number of spins in the sample made it necessary to use a homebuild microwave resonator specifically adapted to the special geometry of the sample—a thin, predominantly two-dimensional conducting sheet on top of a dielectric layer.

This Fabry-Perot-type resonator consists of one spherical mirror opposed to one flat mirror with the normal axis orientated parallel to the magnetic field B_0. It can be operated in various modes with the necessary polarization of the microwave magnetic field $B_1 \perp B_0$. The field distribution of the microwave field is similar to a free plane wave: It has predominantly a transverse polarization with the electrical field perpendicular to the magnetic field. The difference to the free-space situation is that both field components are out of phase by a quarter of a wavelength, which is a decisive advantage for magnetic resonance experiments. More details on this resonator concept can be found in Ref. 9. The applications of Fabry-Perot resonators to W-band ESR spectroscopy are discussed in Ref. 10.

The cross section of the microwave field shows a quasi-Gaussian field distribution with a full width at half maximum of ≈ 5 mm. The flat mirror is also used for supporting the sample that is fixed on it with vacuum grease. For adjusting the resonance frequency of the cavity, the distance between the microwave mirrors can be adjusted in a wide range from 4 to 15 mm by sliding the mirror with a reproducible accuracy of ≈ 1 μm. A shift of 1 μm corresponds to a frequency shift of about 10 MHz, which is somewhat smaller than the bandwith of the resonant mode. For most measurements the best results were obtained with a relatively small distance of 5.0 or 6.6 mm, equivalent to 3 or 4 half wavelengths in the TEM_{003} or TEM_{004} mode.

The lateral dimensions of such flat samples are only restricted by the inner diameter of the modulation coils of 20 mm, which makes it possible to examine samples that are too extended even for conventional X-band cavities. The sample thickness poses a greater problem, because the electrical component E_1 of the microwave field is equal to zero only directly on the surface of the mirror and reaches its maximum value already at a distance of 0.8 mm, corresponding to one quarter wavelength. So clearly the possible sample thickness depends strongly on the electrical properties of the sample, namely on its conductive and/or dielectric losses. The relatively high conductivity of the Si-wafer material and the dielectric properties of Si resulted in too much losses and dramatically reduced the quality factor of the cavity. Therefore, it was necessary to reduce the thickness of the sample by removing as much of the wafer material as possible. Careful mechanical grinding allowed us to reduce the wafer thickness to ≈ 50 μm, sufficient for a reasonable good quality factor of the resonator.

IV. EXPERIMENTAL RESULTS AND DISCUSSION

Recent measurements[6] at a microwave frequency of 9.4 GHz (Fig. 2, X-Band spectrum) essentially resulted in a single Lorentzian shaped line (≈ 0.23 mT half-width at half maximum). A careful analysis of the lineshape showed indications of a second, broader line at nearly the identical field position. A fit to two Lorentzians, however, is not very stable, as the separation of the two lines (≈ 0.1 mT) is smaller than the individual linewidth. In this case the increased g-factor resolution at higher magnetic fields at 94 GHz (W-Band) made it possible to clearly separate the two lines (Fig. 2, W-Band spectrum) and get more reliable values for the line parameters. The g factor is basically a measure of the spin splitting of the electrons in or near the conduction band of Si, defined by $h \cdot f_{\mu w} = g \cdot \mu_B \cdot B_0$. The microwave

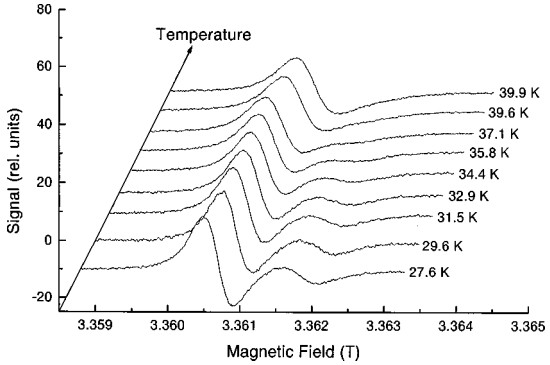

FIG. 3. Behavior of the two lines for increasing temperature. An offset and a shift are added for the clarity of the presentation. Power: 1.3 mW; frequency: 93.97 GHz.

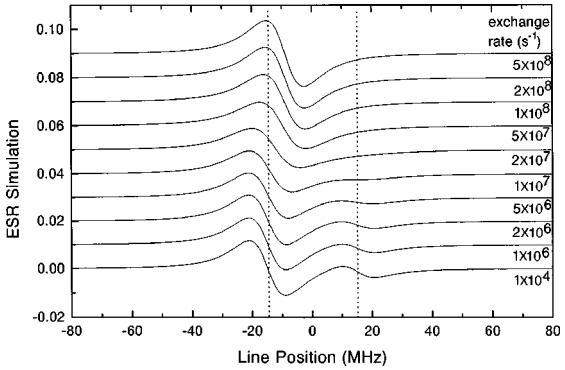

FIG. 4. Simulated lineshapes for the two-site exchange model. The initial separation is 30 MHz, the relative intensities are from the experimental data at $T=27.6$ K.

frequency is denoted by $f_{\mu w}$, μ_B is the Bohr magneton and B_0 is the external magnetic field. The g factors of the two lines at temperatures below 25 K are 1.9993 ± 0.00005 for the stronger and 1.9986 ± 0.00005 for the weaker line, respectively. They are calibrated to the conduction electron g factor of Li metal particles in LiF.[11,12] Weighted with their relative intensities, these values confirm the results published in Ref. 6 and are close to the values obtained for conduction electrons in Si.[13,14] With increasing temperature, the separation of the two lines decreases and above 40 K they merge into one single line with its position at a g factor of 1.9992 ± 0.00005 (Fig. 3).

This general behavior is well known in magnetic resonance and is a clear indication of an exchange between two different spin subsystems that are separated by a specific energy barrier, which can be overcome by thermal activation. Magnetic resonance techniques are particularly sensitive to such exchange processes, if the exchange rate is in the range of the line splitting. In our case the line separation at low temperature is ≈ 30 MHz and the subsequent analysis shows that the ESR signal is very sensitive to exchange rates k in the range $10^4\ \mathrm{s}^{-1}<k<10^8\ \mathrm{s}^{-1}$.

The model used to describe this process is identical to the model for chemical exchange in NMR[15] and is based on electrons located at two different sites (the quantum well and the P donor layer, respectively) that can exchange their magnetization in a kind of jump process. The two spin systems have their individual relaxation times τ_1 and τ_2 and relative magnetizations p_1 and p_2 with $p_1+p_2=1$. The physical mechanism of the jump process is unimportant, but it is assumed to be fast compared to the timescale of the Larmor periods, and it does not lead in itself to relaxation of the spins.

Assuming additionally that both spin systems are essentially homogeneous and can be described by lifetime broadening alone, the lineshape can be calculated analytically. This situation prevails due to either motional and/or exchange narrowing within the spin-subsystems, as evidenced by the predominantly Lorentzian lineshapes. The analytical expression for the lineshape of the resonance with exchange is taken from Ref. 16 and follows the analysis of Ref. 15. Detailed balance requires $p_1\cdot k_{12}=p_2\cdot k_{21}$, where k_{12} and k_{21} are the probabilities for the exchange of magnetization from system 1 to 2 and 2 to 1, respectively. By setting $k_{12}=k(T)/p_1$ and $k_{21}=k(T)/p_2$, we introduce a thermally activated common exchange rate $k(T)$

$$k(T)=k_0\cdot\exp\left(\frac{-\Delta E_a}{kT}\right), \tag{1}$$

where ΔE_a is the activation energy for the process and k_0 is the attempt rate. We denote the line position by $\omega=g\cdot\mu_B\cdot B_0/\hbar$, the frequency positions of lines 1 and 2 as δ_1 and δ_2 and arrive at the expression for the absorption lineshape:

$$I(\omega)=\frac{[p_1\cdot(\omega-\delta_2)+p_2\cdot(\omega-\delta_1)]I_2(\omega)+[\tau_1^{-1}p_2+\tau_2^{-1}p_1+k_{12}+k_{21}]I_1(\omega)}{I_1(\omega)^2+I_2(\omega)^2}, \tag{2}$$

where the $I_i(\omega)$ are defined as

$$I_1(\omega)=(\tau_1^{-1}+k_{12})\cdot(\tau_2^{-1}+k_{21})-(\omega-\delta_1)\cdot(\omega-\delta_2)-k_{12}\cdot k_{21}, \tag{3}$$

$$I_2(\omega)=(\omega-\delta_1)\cdot(\tau_2^{-1}+k_{21})+(\omega-\delta_2)\cdot(\tau_1^{-1}+k_{12}). \tag{4}$$

Since the individual lineshapes are assumed to be homogeneous Lorentzians, the τ_1 and τ_2 have to be identified with the transverse relaxation times and the values are taken from the respective linewidths.

This simulation can be solved with the exchange rate as an adjustable parameter. The results are plotted in Fig. 4 and reproduce all the essential features of the experimental data: At small exchange rates, the model predicts the sum of two

TABLE I. Temperature dependence of the line splitting and of the exchange rate.

Temperature (K)	25	30	32	34	35	36	37	38	39	40
Splitting (MHz)	30.5	29.0	27.0	24.75	23.0	21.25	19.0	16.5	12.5	9.0
Exchange rate (10^6 s^{-1})	0.87	2.8	5.04	7.32	9.19	10.8	13.9	17.4	25.3	35.3

separated Lorentzian lines. With rising exchange rate, the less intense line starts to broaden and shifts first, but the same effect can be seen at higher exchange rates on the more intense line, too. Then both lines form one comparatively broad line with decreasing linewidth for even higher exchange rates. This essential range of the exchange rate extends from 10^6 to 10^8 s^{-1} and includes the value of the line separation (in frequency units). Finally, at higher exchange rates, there is only one Lorentzian-shaped line.

As this model can be solved analytically only for lifetime broadened lines, it is not suitable for a direct fit to the experimental spectra, which are more complicated due to the combined effects of unresolved hyperfine interaction, dispersion contributions due to the electrical conductivity, and different contributions to the linewidth due to only partial motional or exchange narrowing in the spin subsystems themselves. Therefore, we took an alternative approach: We fitted both the simulated and the experimental data by using the same analytical expression (i.e., two Lorentzian lines, with dispersion contribution). In that way, we obtain the intensities, the widths, and the positions of the two lines, only the latter values being important for the analysis of the exchange process. We get two sets of data: The separation of the lines depending on the exchange rate for the simulation on the one hand and the temperature-dependent experimental splittings on the other hand. A comparison of these sets allows us to eliminate the line separation and gives the desired relation between the exchange rate and the temperature.

Table I shows the experimental line separation as a function of the temperature T, taken from the fit of the experimental spectra. The fit of the simulated spectra according to Eq. (2) on the other hand yields the exchange rate as a function of temperature, given in the third line of Table I. In Fig. 5 we plot the exchange rate $\ln[k(T)]$ versus $1/T$, and from a linear regression we obtain an activation energy $\Delta E_a = 19$ meV. Due to the fact that the data points of Fig. 5 are in itself the result of a nonlinear fit both to the experimental data and the simulation, the accuracy of ΔE_a cannot be estimated.

We note that ΔE_a is comparable to the energy difference from E_F to the conduction band edge in the barrier between the quantum well and the doping layer, which was estimated to ≈ 30 meV (see Fig. 1). Therefore, we identify the exchange rate $k(T)$ as monitoring the exchange of magnetization between the quantum well and the P-doping layer, and ΔE_a is the effective energy barrier. Whether the exchange is accomplished by an exchange of electrons (particle and charge exchange) and/or by an exchange of magnetization (spin exchange) cannot be decided by the ESR data alone. We note as well, that the analysis of the ESR experiment is only sensitive to rates $k(T)$ in the range 10^6 $s^{-1} < k(T) < 10^8$ s^{-1}. This ''rate window'' is essentially determined by the initial line separation (≈ 30 MHz in our case). We cannot exclude an additional temperature-independent exchange process (e.g., by tunneling through the barrier), but its rate must be less than $\approx 10^6$ s^{-1}.

One important consequence for the g factors can be seen from Fig. 6, where we plot the g factors of the two individual lines versus T. At low temperature ($T < 20$ K), the lines are clearly separated and we identify the quantum well g factor as $g = 1.9993 \pm 0.00005$, and the g factor of the doping layer as $g = 1.9986 \pm 0.00005$. All experiments on donors and/or conduction electrons in Si so far were unable to resolve these small g factor differences and comparisons of g values to values stated in the literature have to take that into account. We are aware, that both g factors of our experiment are not purely intrinsic values of the Si and the Si:P systems: the g factor of the quantum well depends on the filling with electrons (the Fermi-energy E_F) and on the width of the well. The g factor of the donor layer is a function of the donor concentration and both g values are temperature dependent. Comparisons to theoretical calculations (whether by semiempirical $\mathbf{k}\cdot\mathbf{p}$ or by more refined band-structure calculations) will have to take these details into account. It is not

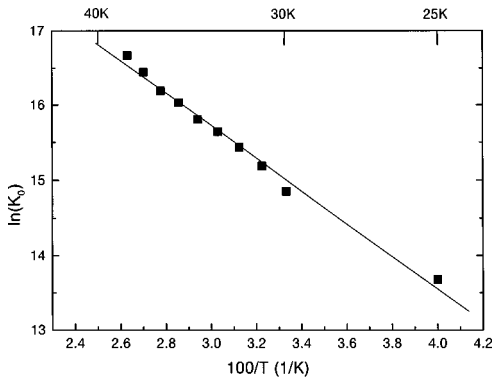

FIG. 5. Exchange rate k as a function of the temperature, taken from a fit to the simulations from Fig. 4.

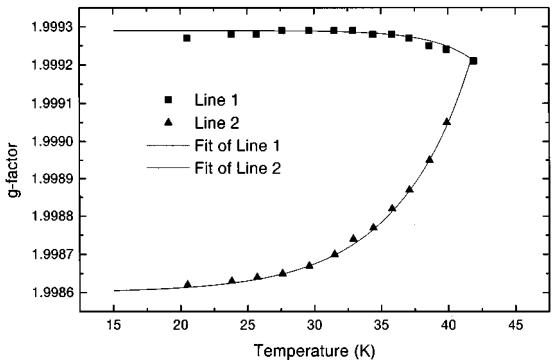

FIG. 6. Temperature dependence of the g factors. The lines are from a fit to the two-site exchange model.

permissible to compare experimental g factors in nanostructured semiconductors to calculations of the g factors of conduction electrons without considering the dependencies analyzed in this contribution.

V. CONCLUSION

We have presented ESR results from $Si/Si_{1-x}C_x$ samples at 94 GHz, which clearly show different contributions to the ESR signal. We were able to interpret the results in a model of exchange between the quantum well $Si_{1-x}C_x$ and the adjacent Si:P doping layers, separated by the energy barrier in the Si spacer layers. The exchange is thermally activated with an activation energy of $\Delta E_a \approx 19$ meV, which is in close agreement with the expected energy barrier obtained from an energy band model. The data shows the important insights obtained from experiments at higher ESR frequencies (higher B_0 fields). The experimental findings are of consequence for the interpretation of g factors in nanostructured semiconductor systems and similar scenarios are expected to prevail in other semiconductor material systems.

ACKNOWLEDGMENTS

We thank K. von Klitzing for stimulating discussions. H.-J. K. acknowledges financial support from the program ''Förderung des wissenschaftlichen Nachwuchses.'' Part of the paper has been financed by DFG Grant No. DE 416/7-1.

*Author to whom correspondence should be addressed.

[1] K. Brunner, K. Eberl, and W. Winter, Phys. Rev. Lett. **76**, 303 (1996).
[2] K. Brunner, W. Winter, and K. Eberl, Phys. Bl. **52**, 1237 (1996).
[3] S. S. Iyer, K. Eberl, M. S. Goorsky, F. K. LeGoues, J. C. Tsang, and F. Cardone, Appl. Phys. Lett. **60**, 356 (1992).
[4] K. Eberl, S. S. Iyer, S. Zollner, J. C. Tsang, and F. K. LeGoues, Appl. Phys. Lett. **60**, 3033 (1992).
[5] W. Faschinger, S. Zerlauth, G. Bauer, and L. Palmetshofer, Appl. Phys. Lett. **67**, 3933 (1995).
[6] N. Nestle, G. Denninger, M. Vidal, C. Weinzierl, K. Brunner, K. Eberl, and K. von Klitzing, Phys. Rev. B **56**, R4359 (1997).
[7] R. L. Williams, G. C. Aers, N. L. Rowell, K. Brunner, W. Winter, and K. Eberl, Appl. Phys. Lett. **72**, 1320 (1998).
[8] B. Radjenovic and D. Tjapkin, Phys. Status Solidi B **156**, 487 (1989).
[9] G. D. Boyd and J. P. Gordon, Bell Syst. Tech. J. **40**, 489 (1961).
[10] R. T. Weber, J. A. J. M. Disselhorst, L. J. Prevo, J. Schmidt, and W. Th. Wenckebach, J. Magn. Reson. **81**, 129 (1989).
[11] A. Stesmans, Phys. Rev. B **47**, 13 906 (1993).
[12] A. Stesmans and G. van Gorp, Rev. Sci. Instrum. **60**, 2949 (1989).
[13] G. Feher, Phys. Rev. **114**, 1219 (1959).
[14] V. Dyakonov and G. Denninger, Phys. Rev. B **46**, 5008 (1992).
[15] A. Abragam, *Principles of Nuclear Magnetism* (Clarendon Press, Oxford, 1961), pp. 447–451.
[16] G. Zimmer, K.-F. Thier, M. Mehring, F. Rachdi, and J. E. Fischer, Phys. Rev. B **53**, 5620 (1996).